

## Electrical resistivity and magnetic behavior of PdNi and CuNi thin films

G. Iannone, D. Zola, A. Angrisani Armenio, M. Polichetti, and C. Attanasio\*

*Laboratorio Regionale SuperMat, CNR-INFM Salerno, and Dipartimento di Fisica "E. R. Caianiello"  
Università degli Studi di Salerno, Baronissi (Sa), I-84081, Italy*

(Received 5 September 2006; revised manuscript received 7 November 2006; published 7 February 2007)

Electrical and magnetic properties of sputtered Pd<sub>86</sub>Ni<sub>14</sub>, Cu<sub>46</sub>Ni<sub>54</sub>, and Cu<sub>42</sub>Ni<sub>58</sub> thin films have been investigated. Pd<sub>86</sub>Ni<sub>14</sub> shows clear ferromagnetic properties even if magnetic clusters of  $4.6\mu_B$  are observed above the Curie-Weiss temperature,  $T_{CW}$ . Different magnetic properties are observed in CuNi alloys. Below  $T_{CW}$ , the field cooling susceptibility increases quasilinearly, while very large magnetic clusters, up to  $10-12\mu_B$ , are observed above  $T_{CW}$ . The temperature behavior of the resistivity of the thin films of the three alloys shows some common features. In particular, after a minimum the resistivity increases, probably due to the scattering of conduction electrons with Ni clusters. The temperature at which the minimum appears does not seem to depend on the host metal (Pd or Cu) and on the Ni concentration. These magnetic clusters affect the resistance behavior in the temperature range where the alloys are paramagnetic or close to their magnetic transition.

DOI: 10.1103/PhysRevB.75.064409

PACS number(s): 75.20.En

### I. INTRODUCTION

During the 1960s, an intense amount of research activity was devoted to the study of transport properties of ferromagnets and ferromagnetic alloys. In particular, a lot of attention was paid to the theoretical and experimental investigation of resistive anomalies near the magnetic transition, and special attention was given to the analysis of the critical exponents close to the magnetic-ordering temperature.<sup>1-8</sup> Effects such as scattering of the conduction electrons by thermal fluctuations due to the spin system or the role of phonons and of lattice expansion have been invoked to explain the experimental data.<sup>9</sup> A big effort was also put into measuring the temperature dependence of the electrical resistivities of different ferromagnetic alloys,<sup>10-14</sup> and there was an attempt to establish a connection between the electrical and magnetic properties of these materials in order to find a criterion to estimate the magnetic-ordering temperature by transport measurements.<sup>15</sup> What essentially came out of these studies was the presence of such anomalies in the  $R(T)$  curves close to the magnetic-ordering temperature,<sup>1</sup> but it was not possible to draw a common interpretation due to the different microscopic mechanisms governing different systems.

Very recently, a renewed interest turned toward weakly ferromagnetic alloys ( $F$ ), such as PdNi and CuNi. In fact, because of the relatively low value of the exchange energy in these systems, they have been largely used in conjunction with superconducting ( $S$ ) materials to realize  $S/F$  layered structures in order to investigate the interplay between superconductivity and ferromagnetism.<sup>16-19</sup> A careful characterization of thin films of these materials is then necessary also because all the previous studies deal with polycrystalline or massive specimens, and, to our knowledge, nothing has presently been reported in the literature dealing with electrical and magnetic properties of PdNi and CuNi thin films having the nickel percentage usually used in the  $S/F$  hybrids. In the case of CuNi, the alloy does not present any magnetic transition below 45% of Ni,<sup>11</sup> and the magnetic-ordering temperature depends strongly on the Ni percentage when the Ni

percentage is in the range between 50 and 60.<sup>18</sup> For these reasons, we decided to study two CuNi alloys with Ni percentage equal to 54 and 58. In addition, because we wanted to study electrical and magnetic properties in Ni-based alloys having similar values for the saturated magnetization, we chose PdNi with Ni percentage equal to 14. In this paper, we report on the electrical and magnetic properties of thin films of PdNi and CuNi prepared by the sputtering deposition technique. We found that while the magnetic behaviors of the chosen Pd- and Cu-based alloys are different, their transport properties look very similar due to the probable formation of Ni clusters.

### II. SAMPLE PREPARATION AND CHARACTERIZATION

Samples were prepared by a magnetically enhanced dc triode sputtering system. The samples were grown on Si(100) substrate held at about 200 °C during the deposition, while the base pressure in the deposition chamber was in the  $10^{-7}$  mbar range, with approximately  $10^{-3}$  mbar of 99.999 purity argon as sputtering gas. The films were deposited at the rate of 0.5 nm/s for PdNi and at 0.6 nm/s for both the CuNi alloys, as controlled by a quartz crystal monitor. The film thickness was also measured by x-ray reflectivity, using a Philips X-Pert MRD high-resolution diffractometer. The reflectivity profiles of a PdNi and a CuNi film are shown, respectively, in Figs. 1(a) and 1(b) together with the simulation curves obtained using the Parrat and Nevot-Croce formalism.<sup>20,21</sup> The fit allows us to obtain the thickness of the samples (see Table I) and the values of the surface roughness, estimated around 0.7 nm for PdNi and 1.2 nm for both of the CuNi alloys. A Pd<sub>1-x</sub>Ni<sub>x</sub> target with  $x=0.10$  was used, but a different Ni concentration, checked by energy dispersive spectrometry (EDS) analysis, was observed in the samples, i.e.,  $x=0.14$ .<sup>19</sup> In the case of CuNi alloys, the estimated concentration measured in the samples is very close to the nominal values of the Ni percentage in the starting targets: Cu<sub>46</sub>Ni<sub>54</sub> and Cu<sub>42</sub>Ni<sub>58</sub>. These analyses were performed on several zones of the samples with typical surface dimen-

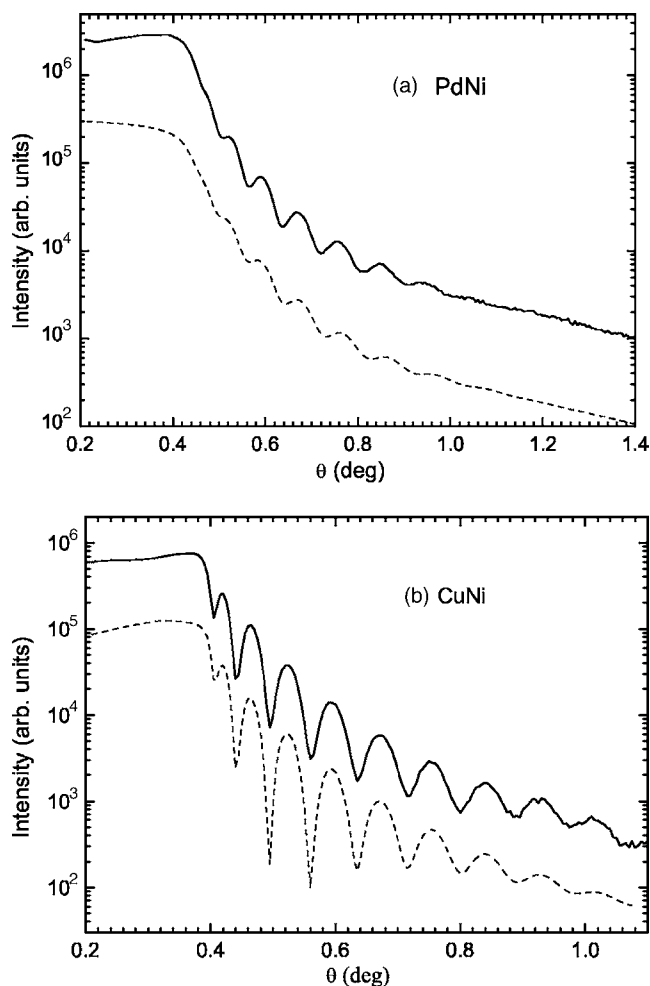


FIG. 1. Experimental (solid line) and calculated (dashed line) low-angle reflectivity profile: (a) 60 nm PdNi14 film; (b) 80 nm CuNi54 film. The numerical simulations are arbitrarily shifted downward for the sake of clarity.

sions of about  $50 \times 50 \text{ nm}^2$ . In the limit of the experimental error, estimated to be less than 3%, measurements show a chemical homogeneity of the films at least on this length scale. In the following sections, we will show the measurements performed on three samples, one for each alloy, namely a  $\text{Pd}_{86}\text{Ni}_{14}$  film (PdNi14) 60 nm thick, a  $\text{Cu}_{46}\text{Ni}_{54}$  film (CuNi54) 80 nm thick, and a  $\text{Cu}_{42}\text{Ni}_{58}$  sample (CuNi58) 50 nm thick.

TABLE I. Thickness ( $d$ ), saturated magnetic moment expressed in Bohr magneton ( $m_{\text{sat}}$ ) at  $T=4.2 \text{ K}$ , effective Bohr magneton ( $p$ ) as estimated from the susceptibility data, coercive field ( $H_C$ ) at  $T=4.2 \text{ K}$ , magnetic ordering temperature ( $T_{\text{CW}}^{\text{RM}}$ ) and Curie-Weiss temperature ( $T_{\text{CW}}$ ) of the analyzed films.  $T_{\text{irr}}$  is defined as the temperature where irreversibility appears in the susceptibility curves.

Sample	$d$ (nm)	$m_{\text{sat}}$ ( $\mu_B/\text{at}$ )	$p$ ( $\mu_B$ )	$H_C$ (Oe)	$T_{\text{CW}}^{\text{RM}}$ (K)	$T_{\text{CW}}$ (K)	$T_{\text{irr}}$ (K)
PdNi14	60	0.21	4.6	620	183	185	172
CuNi54	80	0.15	12	260	220	217	160
CuNi58	50	0.18	10	260	290	295	245

### III. EXPERIMENTAL RESULTS

The resistance versus temperature measurements,  $R(T)$ , have been performed, using the standard four-probe technique, in the temperature range 4.2–350 K. The values of the low-temperature resistivities have been estimated on three deliberately fabricated samples, 60 nm thick, on which a strip  $150 \mu\text{m}$  long and 1 mm wide was obtained by a standard liftoff technique. Typical values for the resistivity were around  $25 \mu\Omega \text{ cm}$  for PdNi and  $50 \mu\Omega \text{ cm}$  for both of the CuNi alloys.

All the magnetic measurements were performed using PPMS 6000 model by Quantum Design equipped with a vibrating sample magnetometer (VSM) operating in the temperature range from 2 K up to 400 K. The field dependence of the magnetic moment,  $m(H)$ , at the temperature of 4.2 K, with the sample surface parallel to the magnetic field, has been preliminarily measured. The measurements, not reported here, show well-formed hysteresis loops, from which the value of the saturation magnetic moment,  $m_{\text{sat}}$ , and the value of the coercive field,  $H_C$ , have been estimated. In order to estimate the value of the magnetic-ordering temperature, the temperature dependence of the remanent magnetic moment,  $m(T)$ , has been measured. The sample was first magnetized at  $T=4.2 \text{ K}$  up to the saturation field, 4 kOe, then the field was lowered down to a remanent field of about 10 Oe, and then the sample was heated until 350 K, describing the upper part of the  $m(T)$  curve. Successively the sample was again cooled down to 4.2 K, describing the lower part of the curve. We define  $T_{\text{CW}}^{\text{RM}}$  as the temperature at which irreversibility appears in the  $m(T)$  curve when cooling down the sample. The saturated magnetic moments and the coercive fields at  $T=4.2 \text{ K}$  and the magnetic ordering temperatures for the three films are summarized in Table I. We have also measured the temperature dependence of the dc susceptibility  $\chi(T)=M/H$  for the three samples. The sample was first cooled down to 4.2 K in zero field, then  $H$  was increased up to 50 Oe, and finally the measurement started describing the lower part of the curve (ZFC). When the temperature reached  $T=350 \text{ K} \gg T_{\text{CW}}^{\text{RM}}$ , the sample was cooled down to 4.2 K giving the higher part of the curve (FC). The Curie-Weiss temperature,  $T_{\text{CW}}$ , has been obtained by fitting the high-temperature data of the susceptibility curve using the expression  $\chi(T)=\chi_0+A/(T-T_{\text{CW}})$ . Here  $\chi_0$  is a constant and  $A=Cp^2$ , where  $p$  is the effective Bohr magneton and  $C=(1/3)(\mu_B^2/k_B)(N/V)$  with  $\mu_B$  the Bohr magneton,  $k_B$  the Boltzmann constant,  $N$  the number of atoms, and  $V$  the volume of the sample. The same procedure has also been applied for the susceptibility data of both the CuNi samples. The obtained  $p$  and  $T_{\text{CW}}$  values are reported in Table I. The  $m(T)$ , together with the  $R(T)$ , and the  $\chi(T)$  measured in the samples PdNi14, CuNi54, and CuNi58, are shown in Figs. 2–4 respectively.

In the PdNi film, we observed a remanent magnetic moment  $m_R$  of  $0.065\mu_B$  at  $T=4.2 \text{ K}$ . It decreases monotonously up to temperatures of around 185 K, which we choose as  $T_{\text{CW}}^{\text{RM}}$ . At this temperature, the magnetic moment  $m$  assumes the value of  $0.008\mu_B$ , which remains constant up to the highest measured temperature. This magnetic moment is prob-

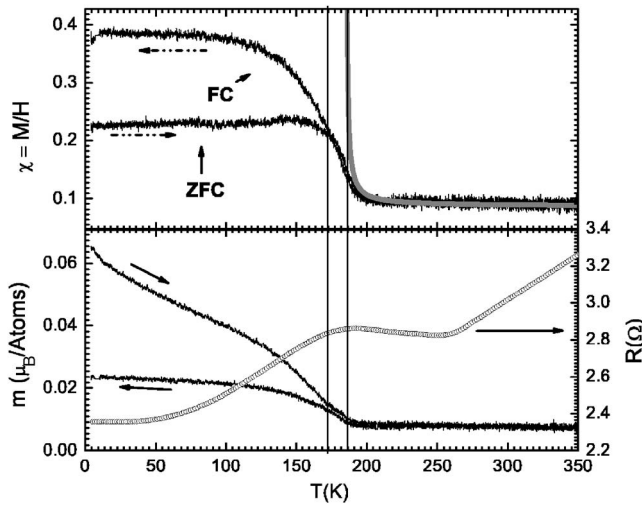


FIG. 2. Lower panel: Magnetic moment as a function of the temperature after saturation at  $T=4.2$  K measured in the PdNi14 film. The electrical resistance ( $R$ ) as a function of temperature (right scale) is also reported. The arrows on the  $m(T)$  curves indicate the measurement sequence. Upper panel: Temperature dependence of the dc susceptibility. The light gray solid line is the fit to the data using the expression for  $\chi(T)$  quoted in the text. The two vertical lines indicate the temperature range where magnetic ordering takes place.

ably due to a very thin layer of segregated nickel caused by the deposition process. In addition, we observe a positive increase of the magnetic moment in the lower branch of the  $m(T)$  curve for temperatures lower than  $T_{CW}^{RM}$ . This behavior is due to the small remanent field entrapped in the VSM

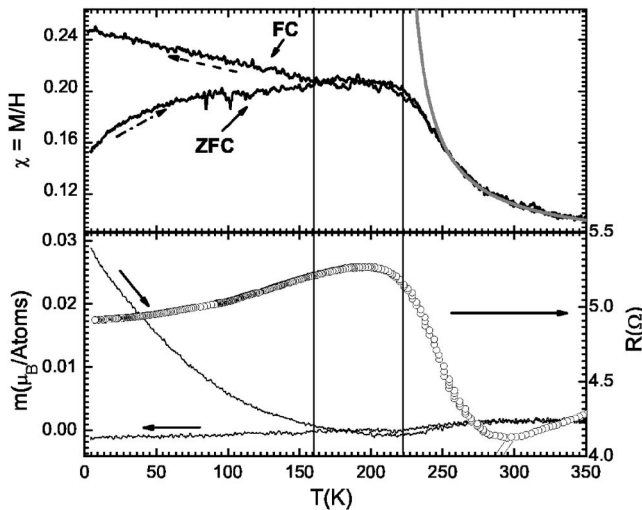


FIG. 3. Lower panel: Magnetic moment as a function of the temperature after saturation at  $T=4.2$  K measured in the CuNi54 film. The electrical resistance ( $R$ ) as a function of temperature (right scale) is also reported. The arrows on the  $m(T)$  curves indicate the measurement sequence. Upper panel: Temperature dependence of the dc susceptibility. The light gray solid line is the fit to the data using the expression for  $\chi(T)$  quoted in the text. The two vertical lines indicate the temperature range where magnetic ordering takes place.

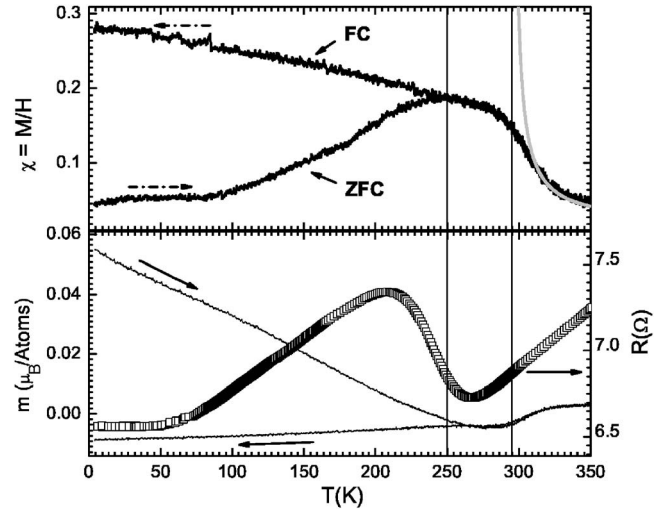


FIG. 4. Lower panel: Magnetic moment as a function of the temperature after saturation at  $T=4.2$  K measured in the CuNi58 film. The electrical resistance ( $R$ ) as a function of temperature (right scale) is also reported. The arrows on the  $m(T)$  curves indicate the measurement sequence. Upper panel: Temperature dependence of the dc susceptibility. The light gray solid line is the fit to the data using the expression for  $\chi(T)$  quoted in the text. The two vertical lines indicate the temperature range where magnetic ordering takes place.

magnet. The Curie-Weiss temperature obtained by fitting the susceptibility data is very close to the  $T_{CW}^{RM}$  evaluated from the  $m(T)$  measurements. The  $\chi(T)$  shows an irreversible behavior for temperatures lower than 172 K and the FC curve saturates for temperatures lower than 100 K. Together with the  $m(T)$  curve, we have reported the  $R(T)$  measurement for the same sample, in the lower panel of Fig. 2. Looking at the figure, we can note, when decreasing the temperature, first a linear decrease up to a minimum value, followed by a slow increase up to a maximum value, and then another linear decrease as a function of the temperature until the saturation value at low temperatures is reached. The position of maximum in the resistance occurs in the temperature range where the magnetic ordering takes place. This region is indicated in the figure by two vertical lines.

A different behavior was observed in the case of the CuNi films where a diamagnetic metal is mixed with a magnetic host. Even if the Ni percentage is above 50% for both samples, the remanent magnetic moments measured in the two alloys at  $T=4.2$  K are, respectively,  $0.029\mu_B$  for CuNi54 and  $0.053\mu_B$  for CuNi58. In the case of CuNi54 (see Fig. 3), the magnetic moment decreases with the temperature and at  $T \approx 175$  K it becomes slightly negative, reaching a minimum value at  $T=220$  K and again zero for  $T=240$  K. The lower branch of the  $m(T)$  curve, i.e., the curve measured cooling the film, crosses the upper curve at the temperature of 180 K and it remains slightly negative. Again, the negative value measured at low temperatures in the lower branch of the  $m(T)$  curve is due to the remanent field entrapped in the VSM magnet, which also affects the behavior of the upper branch. In the susceptibility measurement, reported in the upper panel of Fig. 3, the FC curve is, at higher tempera-



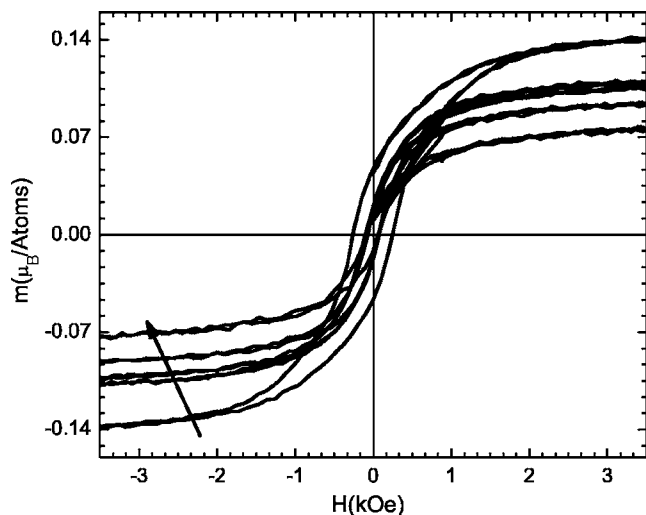


FIG. 5. Magnetization loop for different temperatures for the CuNi54 sample. The values of the temperatures are, starting from the higher value of  $m_{\text{sat}}$ ,  $T=4.2, 150, 170, 200,$  and  $250$  K, as indicated by the arrow.

tures, below the ZFC one and the two branches cross at around 160 K. This seems to be in agreement with the  $m(T)$  results, but major investigations are necessary to clarify the nature of this crossing. Finally, the  $\chi(T)$  show an irreversible behavior for temperature lower than 160 K and the FC curve increases quasilinearly down to the lowest available temperature. Looking at the  $R(T)$  measurements for the same sample, in the lower panel of Fig. 3 we can observe a first linear decrease up to a minimum value, followed by a large increase up to a maximum value, and then another linear decrease in the temperature. The position of the maximum in the resistance occurs for temperatures lower than the estimated  $T_{\text{CW}}^{\text{RM}}$  and in the temperature range where the susceptibility has a reversible behavior.

Even if the magnetic behavior of the CuNi58 film is similar to the CuNi54 sample, in the  $R(T)$  reported in Fig. 4 we can observe that, on the contrary, the maximum occurs in the temperature range where the susceptibility is irreversible, well below the estimated  $T_{\text{CW}}^{\text{RM}}$ . On the other hand, a clear minimum appears in the temperature range where the FC and ZFC susceptibility is reversible. Therefore, the comparison between the magnetic and electric behavior of the two CuNi alloys seems to suggest that it is not possible to set a general criterion to determine the magnetic transition temperature from the resistivity measurements. As far as the susceptibility data are concerned, we can see that they show a reversible behavior in the temperature range from 245 to 290 K, increasing linearly in the FC part as the temperature decreases.

In Fig. 5, we show the  $m(H)$  measurements, recorded at five different temperatures up to  $T=250$  K, for the CuNi54 sample. All the curves have an hysteretic behavior. This fact ensures us that the point at higher temperature at which a reversibility appears and where the two branches of the  $m(T)$  curves intersect each other could be assumed as the magnetic-ordering temperature in the case of the CuNi samples.  $m(H)$  curves similar to those measured in the case of the CuNi54 have been observed also for the CuNi58 film (measurements are not reported here).

To close this section, we wish to comment on the  $m_{\text{sat}}$  values that we obtain from the  $m(H)$  measurements for the three alloys. For PdNi we get  $m_{\text{sat}}=0.21\mu_B/\text{at}$ , in good agreement with values reported in the literature.<sup>22</sup> In the CuNi alloy, the expected saturated magnetization is given by<sup>23</sup>

$$m_{\text{sat}} = m_{\text{sat}}^{\text{Ni}} - (1 - x_{\text{Ni}})(Z_v^{\text{Cu}} - Z_v^{\text{Ni}}), \quad (1)$$

where  $m_{\text{sat}}^{\text{Ni}}$  is the pure Ni saturated magnetization and  $Z_v^{\text{Cu}}$  and  $Z_v^{\text{Ni}}$  are, respectively, the chemical valence of pure elements, i.e., +2 for nickel and +1 for copper. For our Ni concentrations ( $x_{\text{Ni}}=0.54$  and  $0.58$ ), we evaluate, respectively,  $m_{\text{sat}}^{54\%}=0.14\mu_B/\text{at}$  and  $m_{\text{sat}}^{58\%}=0.18\mu_B/\text{at}$ , in good agreement with what we found experimentally.

#### IV. DISCUSSION

It is well known that the correlation between the resistivity and the magnetic properties of ferromagnetic alloys is also related to the contribution of the magnetic scattering that is superimposed to the phononic scattering.<sup>9</sup> In bulk ferromagnetic metals and in many binary alloys, it is found, in a simple picture, that the spin disorder scattering is independent of temperature above  $T_{\text{CW}}^{\text{RM}}$ , whereas it decreases on temperature in the ferromagnetic phase.<sup>24</sup> Since the phononic term decreases on temperature, a clear correlation is usually observed between the magnetic-ordering temperature evaluated from magnetic measurements and a change of slope in the resistivity versus temperature measurements.<sup>24</sup> In the  $R(T)$  measurements performed on the PdNi14 sample, we can observe an effective change of the slope in the region where the ferromagnetic transition appears. Nevertheless, we can observe a slight enhancement of the resistance in the paramagnetic region, around 100 K before the magnetic transition takes place (see Fig. 2). We believe that this behavior is due to the presence of magnetic clusters in our films. In order to test this hypothesis, we analyzed the high-temperature data of the susceptibility employing the Curie-Weiss relation<sup>25</sup> to estimate the effective Bohr magneton  $p$ . In the PdNi14 films we get  $p=4.6\mu_B$ , which is more than three times larger than the estimated value for a pure Pd bulk sample. On a simplified picture of nearly free conduction electrons, the increase in the resistivity could be explained by taking into account the scattering process among these localized magnetic clusters and the free electrons.<sup>26</sup> Indeed, the dimension of a Ni cluster (2–3 nm in diameter for seven Ni atoms) is smaller than the mean free path of the free electrons.

In the case of CuNi, early reports have investigated the resistivity of bulk samples in a wide range of Ni percentage and in a large range of temperature.<sup>11,27,28</sup> In bulk samples, magnetic susceptibility and neutron-scattering measurements have shown the presence of magnetic clusters of 8–12 $\mu_B$  attributed at 20–30 Ni atoms, which means an average cluster dimension of 5–10 nm.<sup>27,28</sup> From high-temperature susceptibility data, we have also estimated the magnetic size of the cluster in the two alloys. In CuNi54 we found 12 $\mu_B$ , whereas 10 $\mu_B$  was obtained for CuNi58, in good agreement with what is reported in the literature.

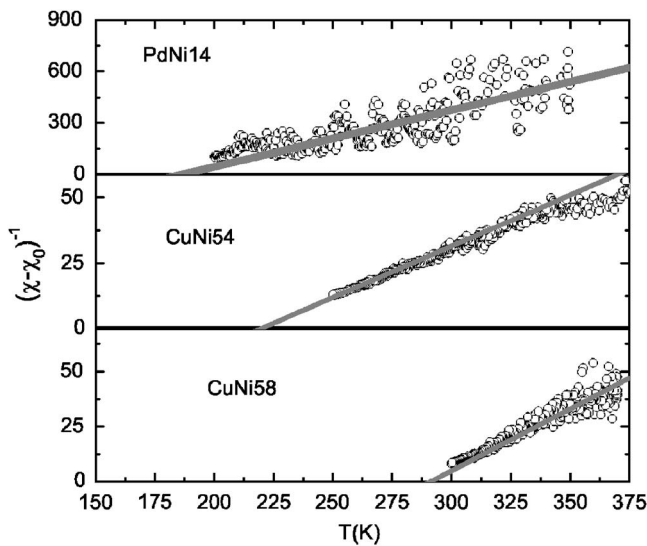


FIG. 6. Temperature dependence of the inverse of the susceptibility for the three measured films. The solid lines are the fits to the experimental data.

In Fig. 6 we show, for the sake of completeness, the fits to the inverse of the susceptibility as a function of the temperature for the three measured films. The estimates for the effective Bohr magnetons and for the Curie-Weiss temperatures are very close to the values previously obtained from the high-temperature susceptibility data.

In bulk samples, the temperature behavior of the resistivity shows a minimum followed by a maximum, for Ni concentration higher than 38%.<sup>11</sup> Nevertheless, the resistivity increases for temperature below 600 K, where the ferromagnetic Ni clusters are probably well formed. Finally, the temperature at which the minimum in the resistivity is observed does not depend on the Ni concentrations.<sup>11</sup> In our films, on the contrary, the minimum in the resistance is observed at around 270 K, well below the bulk value of the nickel fer-

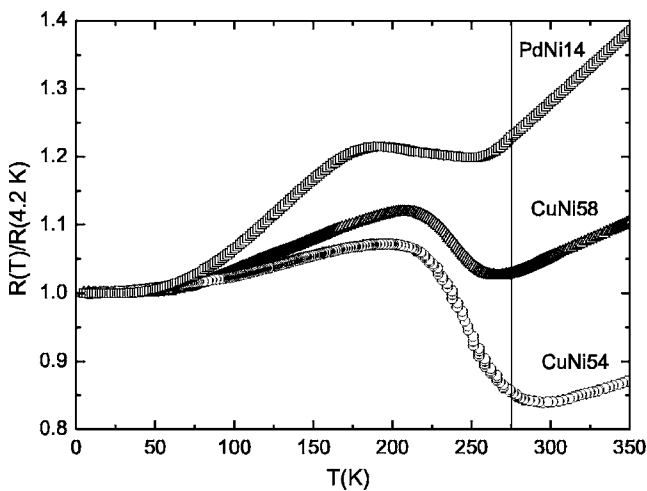


FIG. 7. Temperature dependence of the normalized resistance, at  $T=4.2$  K, for the three analyzed films. The vertical line is a guide to show that the minimum falls at almost the same temperature for the three samples.

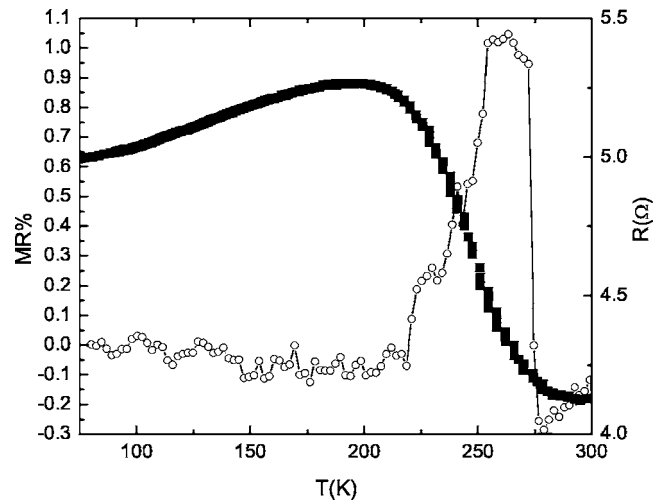


FIG. 8. MR% for the CuNi54 sample at  $H=600$  Oe (left scale). On the right scale is reported the bare measurement of the resistance as a function of the temperature at  $H=600$  Oe.

romagnetic transition temperature. In CuNi58 film, the minimum comes out in the temperature range where the magnetic ordering appears. However, looking at the normalized resistance of the three analyzed films, shown in Fig. 7, we can observe that the minimum falls at almost the same temperature, despite the different magnetic nature of the samples. In order to clarify the presence of cluster scattering in our films, we have also performed magnetoresistance measurements. In Fig. 8, we show for the CuNi54 sample the MR% as a function of the temperature at  $H=600$  Oe. Here  $MR\% = [R(H) - R(0)]/R(0)$ . The result shows that the magnetic scattering is relevant in the region where the Ni clusters are formed, while for temperatures well inside the magnetic phase the MR% is strongly reduced. In Fig. 9, we show the MR% measured at  $T=4.2$  K as a function of the magnetic field for a  $Cu_{42}Ni_{58}$  sample, 10 nm thick. In order to enhance the sensitivity of the measurement, the film has been structured, by a lift-off technique, in a small strip 100  $\mu\text{m}$  long and 10  $\mu\text{m}$  wide. The magnetic field has been applied in the

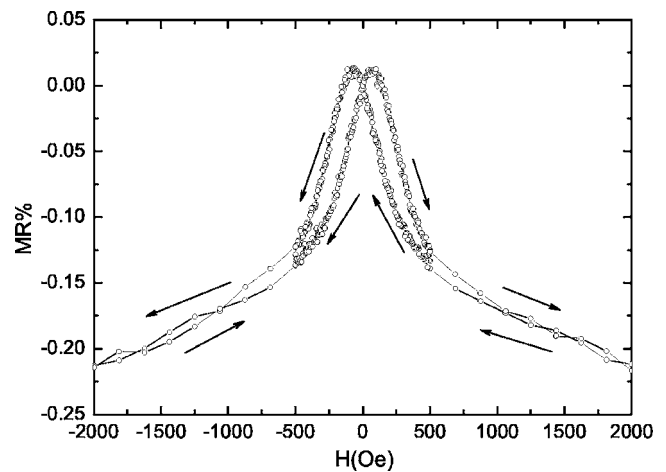


FIG. 9. MR% for a  $Cu_{46}Ni_{54}$  strip at  $T=4.2$  K. The sequence of the measurement is shown by the arrows.

plane of the sample and perpendicular to the direction of the current. Two broad peaks at the coercive fields, characteristic of the anisotropic magnetoresistance, are clearly present due to the presence of magnetic domains. This result confirms that, at low temperatures, the Ni clusters are fully embedded in a magnetic matrix, which completely determines the scattering processes. Very similar results for the MR% have been obtained for the PdNi alloy.

## V. CONCLUSIONS

In this paper, we have analyzed the electrical and magnetic properties of Pd<sub>86</sub>Ni<sub>14</sub>, Cu<sub>46</sub>Ni<sub>54</sub>, and Cu<sub>42</sub>Ni<sub>58</sub> thin films. In the case of PdNi, the magnetic measurements show that the films are ferromagnetic but clustering of Ni atoms is revealed in the paramagnetic phase. The resistivity is affected by a scattering term due to the interaction of free electrons with the magnetic clusters, and this extra scattering is superimposed to the usual spin disorder and to the phonon scatterings. In CuNi thin films we observe a remanent magnetic moment, but much evidence in the remanent magnetic

moment and in the susceptibility as a function of the temperature suggests that the magnetic behavior is not simply ferromagnetic. Large sizes of magnetic clusters are observed in the paramagnetic phase, and the value of the cluster magnetic moment is in good agreement with the reported values in bulk CuNi alloys with a similar Ni percentage. The transport properties seem to be affected by several scattering terms, but the resistivity in the paramagnetic phase increases because of the scattering of the conduction electrons with the magnetic clusters. The formation of these Ni clusters seems to be the cause of the common features observed in the transport properties of the thin films of the three different alloys (at least in the paramagnetic phase and close to the ferromagnetic transition). We did not find any correlation between the change of slope in the temperature dependence of the resistivity and the magnetic transition in the alloys.

## ACKNOWLEDGMENTS

We wish to thank A. Vecchione for x-ray measurements and C. Noce for useful discussions at the early stage of this work.

---

\*Author to whom correspondence should be addressed. Email address: attanasio@sa.infn.it

<sup>1</sup>P. G. de Gennes and J. Friedel, *J. Phys. Chem. Solids* **4**, 71 (1958).

<sup>2</sup>P. P. Craig, W. I. Goldberg, T. A. Kitchens, and J. I. Budnick, *Phys. Rev. Lett.* **19**, 1334 (1967).

<sup>3</sup>M. E. Fisher and J. S. Langer, *Phys. Rev. Lett.* **20**, 665 (1968).

<sup>4</sup>J. A. Mydosh, J. L. Budnick, M. P. Kawatra, and S. Skalski, *Phys. Rev. Lett.* **21**, 1346 (1968).

<sup>5</sup>M. P. Kawatra, S. Skalski, J. A. Mydosh, and J. L. Budnick, *Phys. Rev. Lett.* **23**, 83 (1969).

<sup>6</sup>M. P. Kawatra, J. L. Budnick, and J. A. Mydosh, *Phys. Rev. B* **2**, 1587 (1970).

<sup>7</sup>J. B. Sousa, M. R. Chaves, R. S. Pinto, and M. F. Pinheiro, *J. Phys. F: Met. Phys.* **2**, L83 (1972).

<sup>8</sup>S. Alexander, J. S. Helman, and I. Balberg, *Phys. Rev. B* **13**, 304 (1976).

<sup>9</sup>F. C. Zumsteg and R. D. Parks, *Phys. Rev. Lett.* **24**, 520 (1970).

<sup>10</sup>P. A. Schroeder, R. Wolf, and J. A. Woollam, *Phys. Rev.* **138**, A105 (1965).

<sup>11</sup>R. W. Houghton, M. P. Sarachick, and J. S. Kouvel, *Phys. Rev. Lett.* **25**, 238 (1970).

<sup>12</sup>P. Lederer and D. L. Mills, *Phys. Rev.* **165**, 837 (1968).

<sup>13</sup>S. K. Dutta Roy and A. V. Subrahmanyam, *Phys. Rev.* **177**, 1133 (1969).

<sup>14</sup>D. L. Mills, A. Fert, and I. A. Campbell, *Phys. Rev. B* **4**, 196

(1971).

<sup>15</sup>P. J. Ford and J. A. Mydosh, *Phys. Rev. B* **14**, 2057 (1976).

<sup>16</sup>M. Schöck, C. Sürgers, and H. v. Löhneysen, *Eur. Phys. J. B* **14**, 1 (2000).

<sup>17</sup>T. Kontos, M. Aprili, J. Lesueur, and X. Grison, *Phys. Rev. Lett.* **86**, 304 (2001).

<sup>18</sup>A. Rusanov, R. Boogaard, M. S. B. Hesselberth, H. Sellier, and J. Aarts, *Physica C* **369**, 300 (2002).

<sup>19</sup>C. Cirillo, S. L. Prischepa, M. Salvato, C. Attanasio, M. Hesselberth, and J. Aarts, *Phys. Rev. B* **72**, 144511 (2005).

<sup>20</sup>L. G. Parrat, *Phys. Rev.* **95**, 359 (1954).

<sup>21</sup>L. Nevot and P. Croce, *Rev. Phys. Appl.* **15**, 761 (1980).

<sup>22</sup>T. Kontos, Ph.D. thesis, Université Paris XI (2002).

<sup>23</sup>A. Vernes, H. Ebert, and J. Banhart, *Phys. Rev. B* **68**, 134404 (2003).

<sup>24</sup>Robert C. O'Handley, *Modern Magnetic Material: Principles and Applications* (Wiley Interscience, New York, 2000), p. 557.

<sup>25</sup>C. Kittel, *Introduction to Solid State Physics* (Wiley, New York, 1996).

<sup>26</sup>P. L. Rossiter, *The Electrical Resistivity of Metals and Alloys* (Cambridge University Press, Cambridge, 1987), p. 319.

<sup>27</sup>C. G. Robbins, H. Claus, and P. A. Beck, *Phys. Rev. Lett.* **22**, 1307 (1969).

<sup>28</sup>T. J. Hicks, B. Rainford, J. S. Kouvel, G. G. Low, and J. B. Comly, *Phys. Rev. Lett.* **22**, 531 (1969).